

# Minmax Dynamic Optimization over a Finite-time Horizon for Building Demand Control

H. Sane and M. Guay

**Abstract**—In this paper, we present a real-time dynamic minmax optimization technique over finite-time horizon applied to the building “demand response” problem. The technique is suitable for peak minimization and other types of minmax problems that arise in robust control problems. As in MPC, the optimization algorithm is based on the minimization of a cost function whose minimization provides stability to the closed-loop system. This approach is applied to the peak power demand control problem where electricity consumption and peak power usage in a building has to be controlled in response to real-time pricing. We demonstrate application of this method to a supervisory control problem for building HVAC control that involves minimization of fixed horizon electric utility cost.

**Index Terms**—real-time optimization, minmax optimization, model predictive control, demand response

## I. INTRODUCTION: DEMAND RESPONSE

The minmax real-time optimization problem over fixed-horizon is motivated by the peak power demand response problem where electricity consumption has to be controlled in response to real-time generation capacity and real-time pricing [1]. In electricity grids, demand response (DR) refers to mechanisms to manage the power demand from customers in response to supply conditions, for example, having electricity customers reduce their consumption at critical times or in response to peak market prices. In addition to controlling the energy consumption, there is significant need to reduce peak demand response.[2], [3]. In addition to monthly energy usage cost, the utility providers also charge for peak power usage. The cost to end-use consumer is, therefore, a sum of  $\mathcal{L}_2$  and  $\mathcal{L}_\infty$  norm of power consumption over a fixed month horizon. The power usage is a strong function of the building usage pattern, weather, thermal dynamics and comfort requirements. Therefore, the problem involves real-time control of resources (lighting, HVAC, etc.) in response to model based predictions of energy and utility costs. In demand response, customers, often through the use of dedicated control systems, shed loads in response to a request by a utility or market price conditions.

In this paper, we represent this problem as a real-time dynamic minmax optimization technique over finite-time horizon. Minmax optimization problems also form the basis of most robust model predictive control techniques and differential games. Relatively few algorithms have been

This work was supported in part by the United Technologies Corporate Research.

H. Sane is with the United Technologies Research Center, 411 Silver Lane, East Hartford, CT, USA 06108, M. Guay is with the Department of Chemical Engineering, Queen’s University Kingston, Ontario, Canada K7L 3N6 (email: guaym@chee.queensu.ca)

devised for the solution of minmax dynamic optimization problems. In [4]-[5], a technique for the solution of minmax dynamic optimization problems is proposed. It is shown how one can cast the minmax problem into a standard dynamic optimization problem that is amenable to standard solution techniques. This reformulation can be exploited for the development of real-time minmax algorithms.

In this paper, we use a real-time dynamic minmax optimization technique presented in [6]. The technique, based on the reformulation given in [4], is suitable for peak minimization and other types of minmax problems that arise in robust control problems. As in MPC, the optimization algorithm is based on the minimization of a cost function whose minimization provides stability to the closed-loop system. An interior point method with penalty function is used to incorporate constraints into a modified cost functional, and a Lyapunov based extremum seeking approach is used to compute the trajectory parameters. A precise statement of the numerical implementation of the optimization routine is provided. It is shown how one can take into account the effect of sampling and discretization of the parameter update law.

The layout of the paper is as follows. Section II provides a description of the real-time dynamic optimization technique and its numerical implementation. Some particular implementation issues are discussed in Section III. A brief simulation study is provided in Section IV followed by some brief conclusions.

## II. REAL-TIME DYNAMIC OPTIMIZATION KKK

### A. Minmax dynamic optimization problem

We consider a general class of nonlinear dynamical systems of the form:

$$\dot{x} = f(x, u) \quad (1)$$

where  $x \in \mathbf{R}^n$  are the state variables and  $u \in \mathbf{R}^p$  is the vector of input variables,  $f(x) : \mathbf{R}^n \rightarrow \mathbf{R}^n$  is a smooth continuous functions of  $x$ . There is a vector  $u(t) = [u_1 \dots u_p]$  of  $p$  input variables.

The optimization centers around finding a system trajectory that solves the following minmax dynamic optimization problem:

$$\min_{u(t)} J(u) = \int_0^T q(x(t), u(t)) dt + \max_{t \in [0, T]} F(t, x(t), u(t))$$

subject to

$$\begin{aligned} \dot{x} &= f(x, u) \\ x(0) &= x_0, x(T) = x_f, w(x, u) \geq 0 \end{aligned} \quad (2)$$

where  $F(t, x(t), u(t)) : \mathbb{R} \times \mathbb{R}^n \times \mathbb{R}^p \rightarrow \mathbb{R}^+$  is a smooth function of  $t$ ,  $x$  and  $u$  whose peak value is to be minimized. The constraint function  $w(x, u) : \mathbb{R}^n \times \mathbb{R}^p \rightarrow \mathbb{R}^p$  is assumed to be a smooth vector valued function of  $x$  and  $u$ . The cost functional  $q(x, u) : \mathbb{R}^n \times \mathbb{R}^p \rightarrow \mathbb{R}^+$  is assumed to be smooth and locally convex function of  $x$  and  $u$ . It is assumed that a continuous control,  $u(t)$  exists that can steer the states from  $x_0$  to  $x_f$  over the batch interval  $t \in [0, T]$ . Although  $T$  can be treated as a time-varying parameter, in the following discussion  $T$  is considered to be fixed.

The input trajectories are parameterized

$$u(t) = [ u_1 \quad \dots \quad u_p(t) ] \quad (3)$$

where

$$u_i(t) = \sum_{j=1}^N \theta_{ij} \Xi_{ij}(t) \quad (4)$$

where  $\Xi$  are the basis functions and  $\theta_i$  for  $i = 1, \dots, N$  and  $j = 1, \dots, p$  are the parameters to be determined. The state space equations can be rewritten in terms of  $\theta$  and the initial conditions. If the input is defined as a polynomial then

$$u_i = \theta^T \phi(t) \quad (5)$$

where the parameters and basis functions are expressed as follows

$$\theta = [ \theta_1 \quad \dots \quad \theta_N ] \quad (6)$$

$$\phi(t) = [ 1 \quad t \quad \dots \quad t^{N-1} ]. \quad (7)$$

The vector  $x^p(\tau, t, \theta; x^m(t))$  represents the predicted quantity of the states at time  $\tau$  starting from state  $x^m(t)$  at time  $t$  for  $\tau \geq t$  for the parameter  $\theta$ . In the remainder, the superscript  $m$  denotes a measured quantity, and the superscript  $p$  denotes a predicted quantity. The system of differential equations (1) must be solved to determine  $x^p$ .

Having defined the structure of admissible input trajectories, the dynamic optimization problem can be expressed in terms of the parameters as follows

$$\begin{aligned} \min_{\theta} \quad J(\theta) &= \int_0^T q(x^p(t, 0, \theta; x^m(0)), \theta^T \phi(t)) dt \\ &+ \max_{t \in [0, T]} F(t, x^p(t, 0, \theta; x^m(0)), \theta^T \phi(t)) \end{aligned}$$

subject to

$$\begin{aligned} \dot{x}^p &= f(x^p(t), \theta^T \phi(t)) \\ x^p(0) &= x_0^m \\ x^p(T, 0, \theta; x^m(0)) &= x_f^p \\ w(x^p(t, 0, \theta; x^m(0)), \theta^T \phi(t)) &\geq 0 \end{aligned} \quad (8)$$

The minmax problem must be restated to facilitate the development of a real-time optimization technique. Let  $F^*$  be the unknown maximum value of the function  $F(t, \cdot, \cdot)$ :

$$F^* = \max_{t \in [0, T]} F(t, x^p(t, 0, \theta; x^m(0)), \theta^T \phi(t))$$

Treating this unknown maximum  $F^*$  as a parameter we can rewrite the optimization problem (8) as follows:

$$\begin{aligned} \min_{\theta, F^*} \quad J &= \int_0^T q(x^p(t, 0, \theta; x^m(0)), \theta^T \phi(t)) dt + F^* \\ \text{subject to} \quad & \dot{x}^p = f(x^p(t), \theta^T \phi(t)) \\ & x^p(0) = x_0^m \\ & x^p(T, 0, \theta; x^m(0)) = x_f^p \\ & w(x^p(t, 0, \theta; x^m(0)), \theta^T \phi(t)) \geq 0 \\ & F^* - F(t, x^p(t, 0, \theta; x^m(0)), \theta^T \phi(t)) \geq 0 \end{aligned} \quad (9)$$

The main challenge with this problem remains the minmax problem. The following assumptions are necessary for the design of the real-optimizing predictive controller which solves the optimization problem.

*Assumption 1:* The parameters are assumed to evolve on a compact convex set

$$\Omega_W = \{ \theta \in \mathbb{R}^N \mid \|\theta\| \leq w_m \} \quad (10)$$

where  $w_m > 0$  is a positive constant.

*Assumption 2:* The constraint set

$$\Omega_c = \{ x \in \mathbf{R}^n, u \in \mathbf{R}^p \mid w(x, u) \geq 0, F(t, x, u) \leq F^* \} \quad (11)$$

describes of convex subset of the parameter set  $\Omega_w$ ,  $\forall t \in [0, T]$  and  $\forall F^* \in \mathbb{R}$ .

*Assumption 3:* It is assumed that the input variables evolve on a compact subset  $\Omega$  of  $\mathbf{R}^p$ . The cost functional  $J : \Omega_W \rightarrow \mathbf{R}$  is assumed to be locally convex and Lipschitz continuously differentiable on  $\Omega_W$ . The cost function  $q(x, u)$  is assumed to be sufficiently smooth.

Assumptions 1-3 are needed to handle the parameterized constraints using an interior point method with penalty function. An interior point method incorporating a log barrier function enforces the state and input constraints. The boundary conditions are incorporated through a terminal penalty function. In the remaining equations obvious notation has been omitted.

Let the path cost with the log barrier function be expressed as follows

$$\begin{aligned} L(x^p(t), \theta^T \phi(t)) &= q(x^p(t), \theta^T \phi(t)) \\ &- \sum_{i=1}^{\rho} \mu_i \log(w_i(x^p(t), \theta^T \phi(t)) + \epsilon_i) \\ &- \mu_0 \log(F^* - F(t, x^p(t), \theta^T \phi(t)) + \epsilon_0) \end{aligned} \quad (12)$$

where  $x_p(t) = x^p(t, 0, \theta; x^m(0))$  and where  $\mu_i$  and  $\epsilon_i$  ( $i = 0, 1, \dots, \rho$ ) are strictly positive constants. The new cost functional with interior point inclusion and a penalty function is defined as follows

$$J_{ip} = \int_0^T L(x^p(\tau), \theta^T \phi(\tau)) d\tau + M(x^p(T) - x_f^p)^2 \quad (13)$$

where  $M > 0$  is a strictly positive constants. The tuning parameters of the cost functional are such that  $\mu$  and  $\epsilon$  are taken as small as possible, and  $M$  is taken as large as possible. While the focus of this paper is on convex

problems, so-called infeasible interior-point method can be used to solve nonconvex problems.

### B. Real-time Optimization algorithm

The objective of this study is to develop a real-time algorithm for the solution of minmax dynamic optimization problems, as stated above. To do so, we first decompose the overall cost into two parts. The first part takes into account the cost incurred up to time  $t$ . The second part provides an estimate of the cost-to-go at time  $t$ . A model predictive approach is used to estimate the cost-to-go. The real-time cost estimate at time  $t$  is given by:

$$J_{ip} = \int_0^t L^m(x^m(\tau), u(\tau)) d\tau + \int_t^T L^p(x^p(\tau, t, \theta; x^m(t)), \theta^T \phi(\tau)) d\tau + M(x^p(T, t, \theta; x^m(t)) - x_f^p)^2 \quad (14)$$

The first term represents the actual cost being calculated from the measured states and inputs. The second and third terms give the estimated cost-to-go using the current parameters and the corresponding model predictions,  $x^p(\tau, t, \theta; x^m(t))$ .

A Lyapunov-based approach is used to solve the optimization problem [7]. Assuming that the cost functional is convex with respect to  $\theta$  over  $\Upsilon$ , then the first order conditions can be applied such that at the optimal parameter set  $\theta^*$

$$\nabla J_{ip}(\theta^*) = 0. \quad (15)$$

The Lyapunov function is defined as the cost functional

$$V = J_{ip} \quad (16)$$

and the time derivative is given by

$$\dot{V} = \nabla_{\theta} J_{ip} \dot{\theta} + L^m|_t - L^p|_t \quad (17)$$

By definition  $x^p(t) = x^m(t)$  and ensuring that  $u^p(t) = u^m(t)$  then

$$\dot{V} = \nabla_{\theta} J_{ip} \dot{\theta} \quad (18)$$

Using a straightforward steepest descent approach for the parameter update law

$$\dot{\theta} = -k \nabla_{\theta} J_{ip}. \quad (19)$$

Then the final form of the Lyapunov function is

$$\dot{V} = -k \nabla_{\theta} J_{ip}^T \nabla_{\theta} J_{ip}. \quad (20)$$

The Lyapunov function is strictly decreasing except when the gradient is zero (which occurs at the minima, and at the end of the batch).

To ensure that the parameters remain in the convex set  $\Omega_W$ , a projection algorithm is introduced. The properties of the projection algorithm are discussed in [8]. This algorithm is given as follows

$$\dot{\theta} = Proj(\theta, \Upsilon) = \begin{cases} \Upsilon, & \text{if } \|\theta\| < \omega_n \\ & \text{or } (\|\theta\| = \omega_n \text{ and } \nabla P(\theta) \leq 0) \\ \Psi, & \text{otherwise} \end{cases}$$

where  $\Psi = \Upsilon - \Upsilon \frac{\nabla P(\theta) \nabla P(\theta)^T}{\|\nabla P(\theta)\|_2^2}$ ,  $\Upsilon = -k \nabla_{\theta} J_{ip}$ ,  $P(\theta) = \theta^T \theta - \omega_m \leq 0$ ,  $\theta$  is the vector of parameter estimates and  $\omega_m$  is chosen such that  $\|\theta\| \leq \omega_m$ .

### C. Numerical Implementation

In most applications, it is not possible to solve the optimization problem continuously. One must limit the number of times the gradient information must be updated. Moreover, some form of discretisation of the control action is usually required to account for sampling effects. One simple way to account for this effect is to implement the gradient algorithm via finite difference formula such as a Euler method. This section provides a possible simplification of the optimization routine that operates in a discrete-time framework.

Assume that process measurements are available at intervals of  $\Delta t$ . The most simple finite difference parameter update formula is given by the Euler formula:

$$\theta_{n+1} = \theta_n + \Delta t Proj(\theta_n, \Upsilon_n) \quad (21)$$

where  $\theta_n$  is the value of the parameter updates at time step  $n$  and  $\Upsilon_n = -k \nabla_{\theta_n} J_{ip}(t_{n+1}, x^p(t_{n+1}, \theta_n; x^m(t_n)), \theta_n)$  where  $x^p(t_{n+1}, t_n, \theta_n; x^m(t_n))$  is the prediction of the state variable at time  $t_{n+1}$  computed with initial condition  $x^m(t_n)$ , the state measurement at time  $t_n$ , using the parameter estimate  $\theta_n$ . We will use the notation  $J_n$  to represent the cost  $J_{ip}$  evaluated at time  $t_n$  using parameter estimate  $\theta_n$  with state measurement  $x^m(t_n)$ .

The main advantage of using a simple finite difference approach is to limit the need for the computation of the gradient. Naturally, one must ensure that the choice of  $\Delta t$  provides a reasonable approximation.

The first fundamental question relates to the existence of such a  $\Delta t$  such that  $J_{ip}$  is minimized at each step. This is stated in the following result.

*Theorem 1:* Let the optimization problem stated be such that assumptions 1-3 are satisfied. Then there exists a  $\epsilon^* > 0$  such that  $\forall \Delta t < \epsilon^*$ , the value of  $J_{n+1} < J_n \forall n \in \mathbb{Z}$ .

*Proof:* See [6]. ■

As a consequence of Theorem 1, we get the following feasibility result.

*Corollary 2:* The real-time optimization scheme is feasible if the time required to compute the gradient is less than or equal to  $\epsilon^*$ .

In the next section, we will consider the demand response problem for building HVAC control application and demonstrate the feasibility of the proposed optimization scheme.

## III. BUILDING DEMAND CONTROLS PROBLEM

### A. Plant Description

The plant consists of a building that is equipped with a hydronic plant that supplies chilled water to fan-coil units situated in the building rooms. The building (see Figure 1) consists of five rooms, with four exterior rooms facing different orientations and a interior room, that are subject to various thermal disturbances. The exterior walls exposed to direct and diffused solar irradiation and outside temperature.

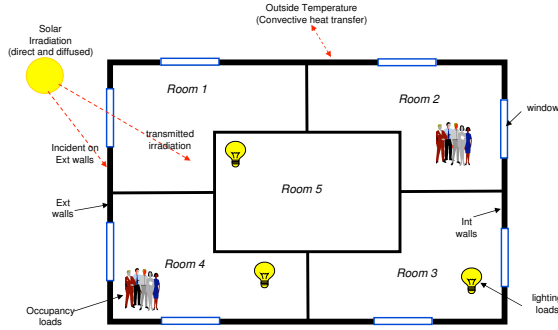


Fig. 1. Layout of the rooms.

Additionally, windows on outer rooms allow a certain fraction of incident solar irradiation into the room. The room is cooled (or heated) by fan-coil units (FCU) that consist of a cross-flow heat exchanger and an electric heater. A fan and a valve controls (see Figure 2) the amount of air and water flowing through the heat exchanger. The room air thermal dynamics is governed by

$$C_{\text{air}} \frac{dT_r}{dt} = Q_{\text{fcu}} + Q_{\text{load}} \quad (22)$$

$$Q_{\text{load}} = k_{wi}(T_{wi} - T_r) + Q_{\text{sol,win}} + Q_{\text{int}} \quad (23)$$

where  $T_r$  is the room temperature,  $T_{wi}$  is interior wall temperature,  $Q_{\text{fcu}}$  is heat-exchanged with the fan-coil unit and  $C_{\text{air}}$  is the thermal mass of air. The heat-transfer rate  $Q_{\text{fcu}}$  is modeled using an  $\epsilon$ -NTU model [9] that depends on the flow-rates and inlet temperature difference of the two fluids. A state-machine and local level PI controller selects the FCU operating mode (heat/cool/off), electric heater toggle, fan speed and valve positions in order to maintain a specified room temperature,  $T_{r,sp}$ . The aggregated heat-load  $Q_{\text{load}}$  entering the room air consists of convective heat from the interior walls  $k_{wi}(T_{wi} - T_r)$ , transmitted solar irradiation  $Q_{\text{sol,win}}$ , and internal heat loads (lights/occupants/equipment)  $Q_{\text{int}}$ . The wall thermal dynamics are given by

$$C_{xi} \frac{dT_{xi}}{dt} = k_{ai}(T_r - T_{xi}) + h_{x1}(T_{xm} - T_{xi}) \quad (24)$$

$$C_{xm} \frac{dT_{xm}}{dt} = h_{x1}(T_{xi} - T_{xm}) + h_{x2}(T_{xo} - T_{xm}) \quad (25)$$

$$C_{xo} \frac{dT_{xo}}{dt} = h_{x2}(T_{xm} - T_{xo}) + k_{ao}(T_{\text{out}} - T_{xo}) + Q_{\text{sol,wall}} + Q_{\text{LW}} \quad (26)$$

where  $T_{xi}$ ,  $T_{xm}$ ,  $T_{xo}$  and  $C_{xi}$ ,  $C_{xm}$ ,  $C_{xo}$  are temperatures and thermal capacities of the interior wall (plaster/gypsum), middle wall (insulation) and exterior wall/ceiling (brick/concrete), respectively. Here,  $T_{\text{out}}$  is the outside air temperature,  $k_{(\cdot)}$  defines the convective heat transfer from wall to air, and  $h_{(\cdot)}$  defines the conductive heat transfer between the wall layers. The longwave radiative heat exchange,  $Q_{\text{LW}}$  is of the form  $\epsilon_{\text{LW}}\sigma_{\text{SB}}(T_{\text{env}}^4 - T_{xo}^4)$ , where  $\epsilon_{\text{LW}}$  is the emmissivity of the outer wall or ceiling,  $\sigma_{\text{SB}}$  is the Stefan-Boltzmann constant, and  $T_{\text{env}}$  is the

effective “environment” temperature for computing long-wave radiation. The chilled water plant (see Figure 2)

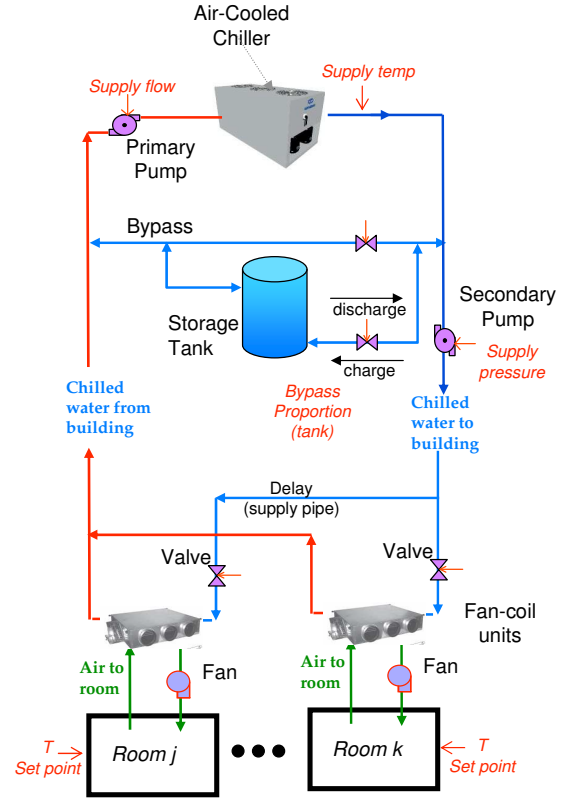


Fig. 2. Schematic of the building HVAC system with supervisory control points highlighted.

consists of a chiller, a primary water pump, a secondary water pump and a chilled water storage tank. The primary pump controls the “primary flow”  $\dot{m}_p$  through the chiller. The secondary pump (secondary flow,  $\dot{m}_s$ ) supplies chilled water to the FCUs using a piping network which introduces variable transport delay that depends on the location of the FCU in the network and the flow-rate. The secondary pump is controlled to provide a fixed pressure drop  $dP_s$  over the building. In case the primary flow is larger than the secondary flow, excess water flow is returned to the chiller through a bypass after mixing with the returned building water. In case the secondary flow is larger than the primary flow, the excess water is returned back to the building after mixing with the primary chilled water supply. A portion of the bypassed flow,  $\dot{m}_b = \dot{m}_p - \dot{m}_s$  can be used to “charge” the chilled water tank in the former case, and “discharge” the tank in the later case. The tank is modeled as a two equal finite volumes, top-tank and bottom-tank, with temperatures  $T_{tt}$  and  $T_{tb}$  which are defined by

$$C_T \frac{dT_{tb}}{dt} = u_T \dot{m}_b c_{pw} (\delta T_{sw} + (1 - \delta) T_{tt} - T_{tb}) + k_{aT} (T_{\text{out}} - T_{tb}) + h_w (T_{tt} - T_{tb}) \quad (27)$$

$$C_T \frac{dT_{tt}}{dt} = u_T \dot{m}_b c_{pw} (\delta T_{tb} + (1 - \delta) T_{r,w,b} - T_{tt}) + k_{aT} (T_{\text{out}} - T_{tt}) + h_w (T_{tb} - T_{tt}) \quad (28)$$

where  $C_T$  is the thermal capacity of half-tank,  $T_{rw,b}$  is the temperature of the building return water,  $T_{sw}$  is the temperature of the supplied water (chiller),  $u_T$  is the fraction of bypass flow  $\dot{m}_b$  which flows through the tank,  $k_{aT}$  defines convective loss to ambient, and  $h_w$  defines the conductive heat transfer between upper and lower water volumes. Here,  $\delta = 1$  in case  $\dot{m}_b > 0$  and  $\delta = 0$  otherwise.

The chiller is a refrigeration system which regulates the supplied chilled water temperature,  $T_{sw,sp}$ . The power consumption of the chiller is modeled as an empirical function of the form,

$$Q_{\text{chiller}} = a_0 + a_1 T_{rw} + a_2 \dot{m}_p + a_3 T_{sw} + a_4 T_{\text{out}} + a_5 T_{sw} T_{\text{out}} + a_6 T_{\text{out}}^2 + a_7 T_{sw}^2 \quad (29)$$

$$P_{\text{chiller}} = b_0 + a_1 T_{rw} + b_2 \dot{m}_p + b_3 T_{sw} + b_4 T_{\text{out}} + b_5 T_{sw} T_{\text{out}} + b_6 T_{\text{out}}^2 + b_7 T_{sw}^2 \quad (30)$$

where  $T_{rw}$  is the temperature of the water entering the chiller,  $T_{sw}$  is the temperature of the supplied chilled water,  $Q_{\text{chiller}} = \dot{m}_p c_{pw} (T_{sw} - T_{rw})$  is the cooling provided, and  $P_{\text{chiller}}$  is chiller power consumption. Note that,  $T_{rw}$  is the temperature of the water after bypass and building return mix, in case  $\dot{m}_b > 0$ .

### B. Fixed horizon MPC Problem

We consider a problem of fixed-horizon predictive control of setpoints of various HVAC equipments (see Figure 2) in a building. The total cost is the fixed-horizon (e.g. monthly) electric bill (\$) that consist of a weighted integral of the power consumption, weighted maximum of peak-time power usage, and a weighted maximum of off-peak-time power usage. Let  $P$  be the total power consumed by the chiller, primary pump, secondary pump, electric heater and fans in the fan-coil units,  $w_e(t)$  be the energy-rate in \$/kWhr,  $w_p(t)$  and  $w_{op}(t)$  are peak and off-peak demand charge in \$ per peak kW. Using notation in (2), the cost is given by

$$J(u) = \int_0^T w_e(t) P(x(t), u(t)) dt + \max_{t \in [0, T]} w_p(t) P(x(t), u(t)) + \max_{t \in [0, T]} w_{op}(t) P(x(t), u(t)) \quad (31)$$

where the control input  $u = [u_1, u_2, u_3, u_4, u_5]^T$ , where  $u_1 = \dot{m}_p$  is the primary flow set-point,  $u_2 = T_{sw,sp}$  is chiller supply water temperature setpoint,  $u_3 = T_{r,sp}$  is room temperature setpoint,  $u_4 = dP_s$  is secondary pump pressure drop setpoint, and  $u_5 = u_T$  is chilled storage tank flow fraction. The objective is to minimize  $J(u)$  over the fixed horizon  $T$  subject to interval control constraints of the form  $u_i \in (u_{i,low}, u_{i,high})$ , where  $u_{i,low}$  and  $u_{i,high}$  could be time varying. For numerical simplification, we used normalized control variables  $\tilde{u}_i$  with respect to upped and lower bounds, so that  $\tilde{u}_i = (u_{i,high} - u_i) / (u_{i,high} - u_{i,low})$  and  $\tilde{u}_i \in (0, 1)$ .

### C. Parametrization

In this paper, we first consider the simplest possible parametrization where each input assumed to remain con-

stant. Given the real-time nature of the optimization algorithm, the resulting controls will be time varying but the optimization part is performed subject to a constant input parametrization. More elaborate parametrizations can be incorporated in this framework. Two minimax parameters must be added to the optimization to account for the contributions of peak cost and off-peak cost to the overall energy cost for the building.

### D. Results

In our numerical example, the chilled water plant consists of a 18kW chiller with a primary nominal flow rate of 0.55 kg/s, FCUs with nominal capacity of 3.2 kW and a 1  $m^3$  chiller water tank. The solar loads and ambient conditions are extracted from the TMY database for Hartford, CT in the months of July. Typical outside air temperature and solar irradiation densities are shown in figures 3 and 4, respectively. The rooms are of size 10m $\times$ 8m $\times$ 4m with interior walls, insulation and exterior brick wall. The internal load schedule including lights, equipment and room-occupancy are chosen to correspond to a typical office application (8am-6pm). For  $u_3 = T_{r,sp}$  we consider that the upped and lower bounds are dynamic based on the occupancy schedule for the building, and are shown in Figure 5.

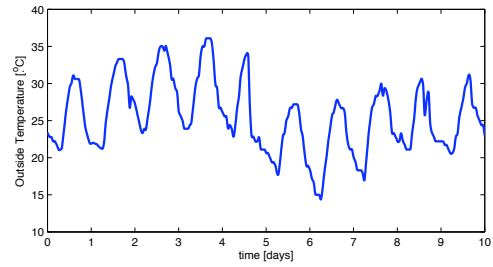


Fig. 3. Typical outside air temperature  $T_{\text{out}}$ .

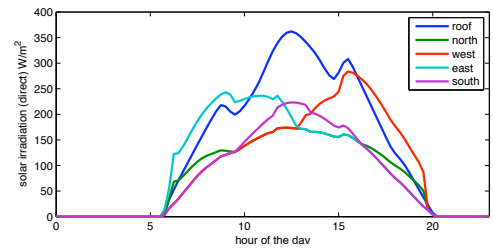


Fig. 4. Incident solar irradiation density (typical day)  $Q_{\text{solar}}$ .

For demonstration purposes, we consider a fixed horizon of  $T = 15$  days. In our case, we choose an energy rate  $w_e(t)$  as shown in Figure 6, peak demand charge of  $w_p(t) = \$14.5$  per peak kW during the peak hours of 2pm-6pm and zero elsewhere, and off-peak demand charge of  $w_{op}(t) = \$4.5$  per peak kW during the off-peak hours and zero elsewhere.

The real-time optimization approach was implemented in a one-day simulation. The nominal cost of the problem is computed using the following input values:  $u_1 = 1, u_2 = 280.15, u_3 = 297.15, u_4 = 1, u_5 = 0.4$ . The worst case

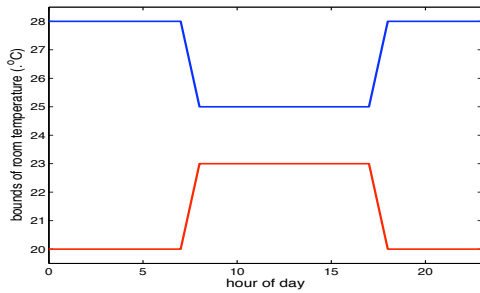


Fig. 5. Dynamic constraints on temperature  $u_3 = T_{r,sp}$ .

peak cost was fixed at 70 and the off-peak cost at 22. These values were used as initial estimates for the real-time optimization technique. The nominal cost was computed using standard log-barrier functions for the worst case costs. Input constraints could simply be enforced using a projection algorithm in this case.

Figure 7 shows the decrease of the cost functional with time. A sampling time of one hour was used in this case. It is important to note that the total cost optimized is composed of the past cost and the future cost at any given point in time. The final cost is the actual cost incurred by the process. The results show a steady decrease of the cost. Figure 8 shows the resulting control action. A final value of 1.81 was obtained. The off-peak cost and peak cost obtained are given by 19.3 and 14.0, In comparison, the nominal energy cost obtained was given by 4.1 and the off-peak and peak costs were 61.1 and 17.5. Results demonstrate that the real-time optimization procedure can provide significant reductions in energy costs despite a rather coarse sampling regime and a simplistic parametrization. For the purpose of this paper, we have limited ourselves to a simpler example. A more detailed simulation study will be provided involving a more elaborate parametrization evaluated over a 15 day period.

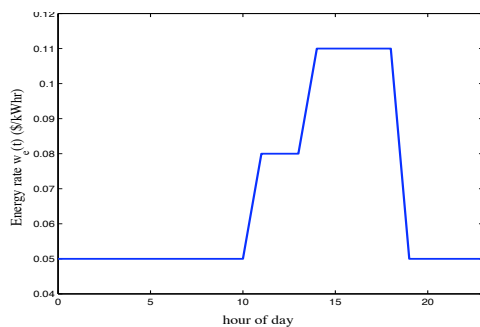


Fig. 6. Energy rate  $w_e(t)$  in (31).

#### IV. CONCLUSION AND FUTURE WORK

In this paper, we applied a real-time dynamic optimization technique developed for a class of minmax optimization problems to a building demand response problem. Smooth trajectories were generated on-line with feasible computing time to construct optimal trajectories without the need for off-line analysis. In future work, we plan to study the impact

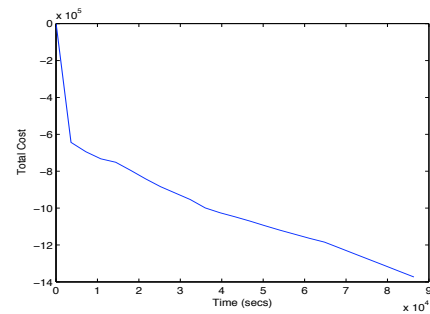


Fig. 7. Total cost from the real-time optimization routine.

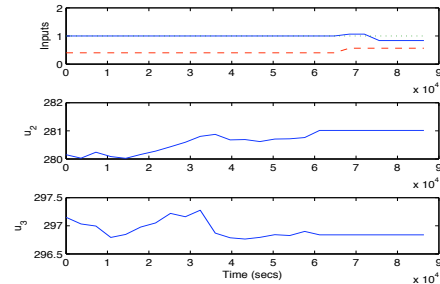


Fig. 8. Control inputs from the real-time optimization routine. The top graph shows inputs  $u_1$  (full line),  $u_4$  (dotted line) and  $u_5$  (dashed line). The middle graph shows input  $u_2$  and the bottom,  $u_3$ .

of imperfect state measurements and parametric uncertainties.

#### V. ACKNOWLEDGMENTS

The authors gratefully acknowledge the support of United Technologies Research Center.

#### REFERENCES

- [1] S. Kiliccote, M. Piette, and D. Hansen, "Advanced controls and communications for demand response and energy efficiency in commercial buildings," LBNL, Tech. Rep. 59337, January 2006.
- [2] M. Piette, D. Watson, N. Motegi, S. Kiliccote, and P. Xu, "Automated critical peak pricing field tests: Program description and results," LBNL, Tech. Rep. 59351, April 2006.
- [3] M. Brambley, D. Hansen, P. Haves, and D. Holmberg, "Workshop results, DOE advanced controls R&D planning workshop," Washington D.C., June 2003, available at [http://www.eere.energy.gov/buildings/tech/controls/pdfs/pnml-15148\\_workshop.pdf](http://www.eere.energy.gov/buildings/tech/controls/pdfs/pnml-15148_workshop.pdf).
- [4] A. Miele, B. Mohanty, P. Venkataraman, and Y. Kuo, "Numerical solution of minimax problems of optimal control, part 1," *Journal of Optimization Theory and Applications*, vol. 38, no. 1, pp. 97–109, September 2001.
- [5] —, "Numerical solution of minimax problems of optimal control, part 2," *Journal of Optimization Theory and Applications*, vol. 38, no. 1, pp. 111–135, September 2001.
- [6] M. Guay and H. Sane, "Model predictive control for on-line optimization of semi-batch reactors," in *Proceedings of the American Control Conference*, July 2007, pp. 1233–1238.
- [7] M. Guay and N. Peters, "Real-time dynamic optimization of nonlinear systems: A flatness-based approach," in *Proc. IEEE CDC-ECC 2005*, 2005.
- [8] M. Krstic, I. Kanellakopoulos, and P. Kokotovic, *Nonlinear and Adaptive Control Design*, J. Wiley and Sons, Eds., 1995.
- [9] J. P. Holman, *Heat Transfer*, 9th ed. Princeton, NJ: McGraw-Hill, 2001.